Journal of Hazardous Materials 176 (2010) 418–425

Contents lists available at ScienceDirect

Journal of Hazardous Materials

journal homepage: www.elsevier.com/locate/jhazmat

Cr(VI) reduction in wastewater using a bimetallic galvanic reactor

Violeta Lugo-Lugo[a], Carlos Barrera-Díaz[a,*], Bryan Bilyeu[b], Patricia Balderas-Hernández[a], Fernando Ureña-Nuñez[c], Víctor Sánchez-Mendieta[a]

[a] Centro Conjunto de Investigación en Química Sustentable UAEM-UNAM. Universidad Autónoma del Estado de México. Facultad de Química. Paseo Colón intersección Paseo Tollocan S/N. C.P. 50120, Toluca, Estado de México, Mexico
[b] Xavier University of Louisiana, Department of Chemistry, 1 Drexel Drive, New Orleans, LA 70125, United States
[c] Instituto Nacional de Investigaciones Nucleares, A.P. 18-1027, Col. Escandón, Delegación Miguel Hidalgo, C.P. 11801, México, D.F., Mexico

ARTICLE INFO

Article history:
Received 31 July 2009
Received in revised form 28 October 2009
Accepted 8 November 2009
Available online 13 November 2009

Keywords:
Electrochemical
Wastewater
Hexavalent
Chromium
Chromate
Heavy metal

ABSTRACT

The electrochemical reduction of Cr(VI)–Cr(III) in wastewater by iron and copper–iron bimetallic plates was evaluated and optimized. Iron has been used as a reducing agent, but in this work a copper–iron galvanic system in the form of bimetallic plates is applied to reducing hexavalent chromium. The optimal pH (2) and ratio of copper to iron surface areas (3.5:1) were determined in batch studies, achieving a 100% reduction in about 25 min. The Cr(VI) reduction kinetics for the bimetallic system fit a first order mechanism with a correlation of 0.9935. Thermodynamic analysis shows that the Cr(VI) reduction is possible at any pH value. However, at pH values above 3.0 for iron and 5.5 for chromium insoluble species appear, indicating that the reaction will be hindered. Continuous column studies indicate that the bimetallic copper–iron galvanic system has a reduction capacity of 9.5890 mg Cr(VI) cm^{-2} iron, whereas iron alone only has a capacity of 0.1269 mg Cr(VI) cm^{-2}. The bimetallic copper–iron galvanic system is much more effective in reducing hexavalent chromium than iron alone. The exhausted plates were analyzed by SEM, EDS, and XRD to determine the mechanism and the surface effects, especially surface fouling.

1. Introduction

Heavy metals exist in the wastewater discharge of many industries among which the plating facilities, tanneries and mining operations are especially prominant. Hexavalent chromium is of particular concern because it is carcinogenic and mutagenic, diffuses quickly through soil and aquatic environments, is a strong oxidizing agent, and irritates plant and animal tissues in small quantities [1,2]. In aqueous solutions, Cr(VI) usually exists as $Cr_2O_7^{2-}$, CrO_4^{2-} and $HCrO_4^-$, the relative distribution of which depends on the solution pH and concentration [3,4]. However, none of them form insoluble compounds, so separation by precipitation is not feasible [5]. While Cr(VI) oxyanions are very mobile and toxic in the environment, Cr(III) cations are not. Like many metal cations, Cr(III) forms insoluble precipitates. Thus, reducing Cr(VI)–Cr(III) simplifies its removal from effluent and also reduces its toxicity and mobility [6].

The most widely used industrial method for Cr(VI) removal requires three steps: the addition of sulfuric acid (H_2SO_4) to adjust the pH of the wastewater to a value of 2–3, the addition of a soluble iron salt ($FeCl_2$ or $FeSO_4$) or sodium bisulphate ($NaHSO_3$) for the chemical reduction, and finally a pH adjustment up to about 9 to form the precipitate. While this method is effective, it requires a large amount of chemical reagents and energy and produces a considerable amount of sludge [7–9].

A novel approach for Cr(VI) reduction is the use of direct electrochemical methods, since they provide good reduction yields, require fewer chemicals, and produce less sludge. These direct methods generate reactive species or surfaces by applied currents and have attracted a great deal of attention because of their versatility and environmental compatibility, which makes the treatments of liquids, gases, and solids possible. In fact, the main reagent is the electron, which is a "clean reagent" [10–13].

We have previously reported that Fe(II) ions can be electrochemically produced from steel anodes, which then reduce Cr(VI)–Cr(III) which are precipitated by pH adjustment [14]. Electrochemical reduction with graphite-packed electrodes reduces 94% of the hexavalent chromium in solution [15]. When reticulated vitreous carbon electrodes were used, that value increases to 100% [16,17]. However, in all these cases the electrolysis requires energy input into the system.

A system that does not need external energy to produce metal ions is the galvanic or bimetallic system, like that used in cathodic

* Corresponding author. Tel.: +52 722 2766611; fax: +52 722 2766639.
E-mail address: cbarrera@uaemex.mx (C. Barrera-Díaz).

0304-3894/$ – see front matter © 2009 Elsevier B.V. All rights reserved.
doi:10.1016/j.jhazmat.2009.11.046

and anodic protection. Cathodic protection has been employed for many years to prevent the corrosion of metals. The principles may be explained by considering the corrosion of a typical metal (M) in an acidic environment. The electrochemical reactions which occur are the dissolution of the metal and the evolution of hydrogen gas:

$$M \rightarrow M^{n+} + ne^{-} \quad (1)$$

$$2H^{+} + 2e^{-} \rightarrow H_2 \quad (2)$$

Cathodic protection is achieved by supplying electrons to the metal to be protected. Eqs. (1) and (2) indicate that the addition of electrons to the metal will suppress the metal dissolution and increase the rate of hydrogen evolution. There are two ways to cathodically protect a metal: by an external power supply or by appropriate galvanic coupling [18]. Galvanic protection involves coupling the protected metal with a more active metal with a higher reduction potential, so that the more active metal is preferentially oxidized. The active metal serves as the anode in the electrochemical couple. This anode is called a sacrificial anode since it is consumed. The oxidation and dissolution of the sacrificial metal is faster in a galvanic couple than it would be individually. Likewise, in a traditional galvanic cell, the anode will dissolve while the cathode may grow.

Since the objective is to produce Fe(II) ions which will reduce the Cr(VI) ions in the solution, the copper–iron couple is used to enhance the oxidation of the iron in the system. Like a galvanic cell battery the process is powered by the potential difference between the two metals, so no external energy is required. Thus, the system is self-contained and portable for operation in remote locations.

2. Materials and methods

2.1. Chromium(VI), chromium(III), copper and iron analysis

Synthetic wastewater solutions with Cr(VI) concentrations of 10 and 100 mg L^{-1} were prepared with reagent-grade potassium dichromate in distilled water and adjusted to pH values between 2 and 10 with H_2SO_4 and NaOH. These solutions were treated with iron and iron–copper bimetallic plates. At regular time intervals, the solutions were analyzed for Fe, Cu, and Cr which was further differentiated between Cr(VI) and Cr(III). The total concentrations of chromium, copper and iron in the supernatant liquid samples were determined by atomic absorption spectroscopy using a Varian SpectrAA spectrophotometer model 10-plus. Cr(VI) concentration was measured using the 1–5 diphenylcarbazide method (AWWA 3500-Cr D colorimetric method) with a HACH DR 4000 spectrophotometer at 540 nm. Thus, the Cr(III) concentration was calculated as Cr(III) = total Cr − Cr(VI). In all cases the standard methods from AWWA were followed [19].

2.2. Corrosion tests

The rate of iron corrosion (oxidation) in the Cr(VI)/Fe redox reaction as a function of the copper–iron surface area ratio was measured using a three-electrode glass cell connected to an Autolab potentiostat model PGSTAT302N controlled by a PC. The system employs a platinum counter electrode, a calomel reference electrode, and a PTFE-sealed carbon steel rod (AISI-SAE 1018) working electrode. The exposed surface area of the working electrode was 0.04524 cm^2. The electrodes were abraded with fine emery paper, polished with alumina powder, and finally rinsed with distilled water and then the working electrode was mounted into a PTFE holder which controlled the surface area exposed to the solution. The working electrode was connected to copper rods with different surface areas (copper–iron surface area ratios = 0, 2, 3.5 and 5.5) in order to determine the influence of the cathodic area on the corrosion rate. Measurements were performed in an aqueous solution of 10 mg/L Cr(VI) solution adjusted to pH 2 by adding sulfuric acid. The rate of corrosion induced by the bimetallic contact was determined by linear sweep voltammetry, which measures the extent of polarization over a potential range of −0.02 V to 0.02 V at a rate of 1 mV s^{-1}.

2.3. Batch reactor experiments

Batch reduction tests were carried out on the Cr(VI) solutions using iron, copper and copper–iron bimetallic plates as electrochemical systems with an area of 2 cm^2. The plates were abraded with fine emery paper, polished with alumina powder, and rinsed with distilled water, then brought into contact with 20 mL of 10 mg L^{-1} Cr(VI) solution. All experiments were conducted at room temperature (18 ± 0.5 °C) at specified pH values.

2.4. Continuous Cr(VI) reduction

To evaluate the continuous Cr(VI) reduction in the systems three packed columns were constructed of 14 mm × 70 mm × 0.7 mm parallel iron, copper or copper–iron bimetallic plates, with a total area of 784 cm^2 as shown in Fig. 1.

All column tests were done on a 100 mg L^{-1} aqueous Cr(VI) solution with an initial pH of 2 at an influent-rate of 1 mL min^{-1}. To clean the plates, the column was washed prior to each experiment with an acid solution and rinsed with distilled water. Column effluent samples were withdrawn at regular volume intervals and analyzed for the concentrations of total chromium and Cr(VI), in the supernatant liquid samples using atomic absorption spectroscopy and the diphenylcarbazide method described above. These results were used to calculate the reduction capacity.

2.5. Thermodynamic analysis

In this work, the method for the construction of predominance-zone diagrams and Pourbaix diagrams was based on methodology previously reported [20,21].

2.6. Characterization of iron and copper–iron plates

After the process, the iron and copper plates were imaged by scanning electron microscopy (SEM) using a JEOL-5900-LV at 20 keV to determine the topographical surface changes and characterized by energy dispersive X-ray spectroscopy (EDS) for semi-quantitative elemental analysis. X-ray diffraction (XRD) was done on all the materials before and after the Cr(VI) reduction using a SIEMENS D-5000 diffractometer.

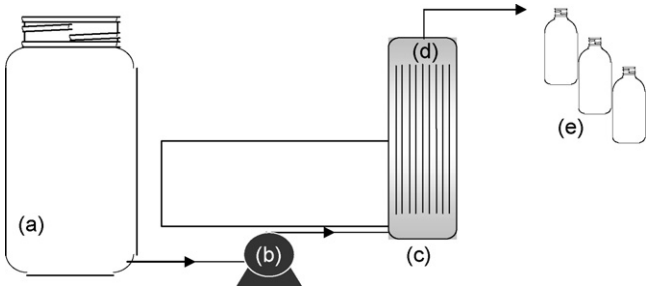

Fig. 1. Experimental setup: (a) storage influent Cr(VI) solution tank; (b) peristaltic pump; (c) packed column; (d) iron or copper–iron square plates; (e) storage effluent bottles.

3. Results and discussion

3.1. Corrosion tests: optimization of surface areas

To optimize the ratio of copper to iron in the bimetallic mixture which reduces Cr(VI) through iron corrosion (oxidation), the current density J_{corr} (A cm^{-2}) is related to the overpotential η (V) at different ratios, as shown in Fig. 2a. Since the overpotential is related to the activation energy of the electron transfer of the redox reaction and higher overpotentials generate the higher reaction rates reflected by higher current densities, the reaction kinetics are shown in the relationship between current density and overpotential. As shown in Fig. 2a, the rate of the Cr(VI)/Fe redox reaction reflected in the slope of the current density vs. overpotential graph increases as the copper–iron ratio increases from 0 to 3.5, but does not increase beyond that. Therefore, 3.5 is the optimum ratio of copper to iron surface areas and the reactor was constructed using this ratio.

The current density J_{corr} (A cm^{-2}) as a function of time (min) for different copper to iron surface area ratios is shown in Fig. 2b. In all systems, the current density decreases from a high initial value to a stable equilibrium value within about 20 min. The equilibrium current densities increased with increasing copper to iron surface ratios.

3.2. Cr(VI) reduction in batch mode

Fig. 3 shows Cr(VI) reduction by copper–iron bimetallic galvanic plates, iron and copper at different pH values. At pH 2, both plates copper–iron and iron quickly and completely reduced the Cr(VI). The copper plates also reduce the Cr(VI) completely, but at fewer

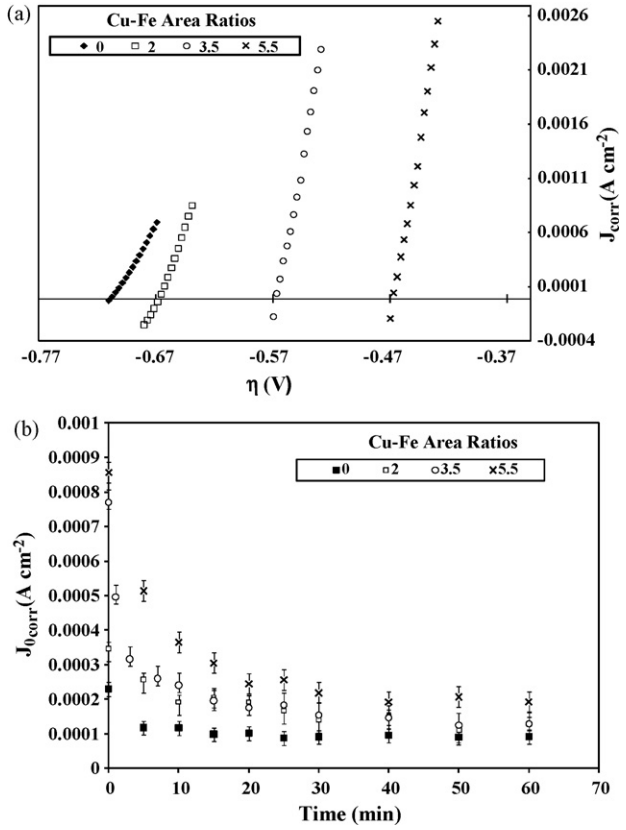

Fig. 2. (a) Overpotential η vs. current density J_{corr} (A cm^{-2}) for determining rate of Cr(VI)/Fe redox reaction in the iron–copper galvanic systems and (b) current density as a function of exposed time, both for different copper–iron surface area ratios in a 10 mg L^{-1} Cr(VI) solution at pH 2.

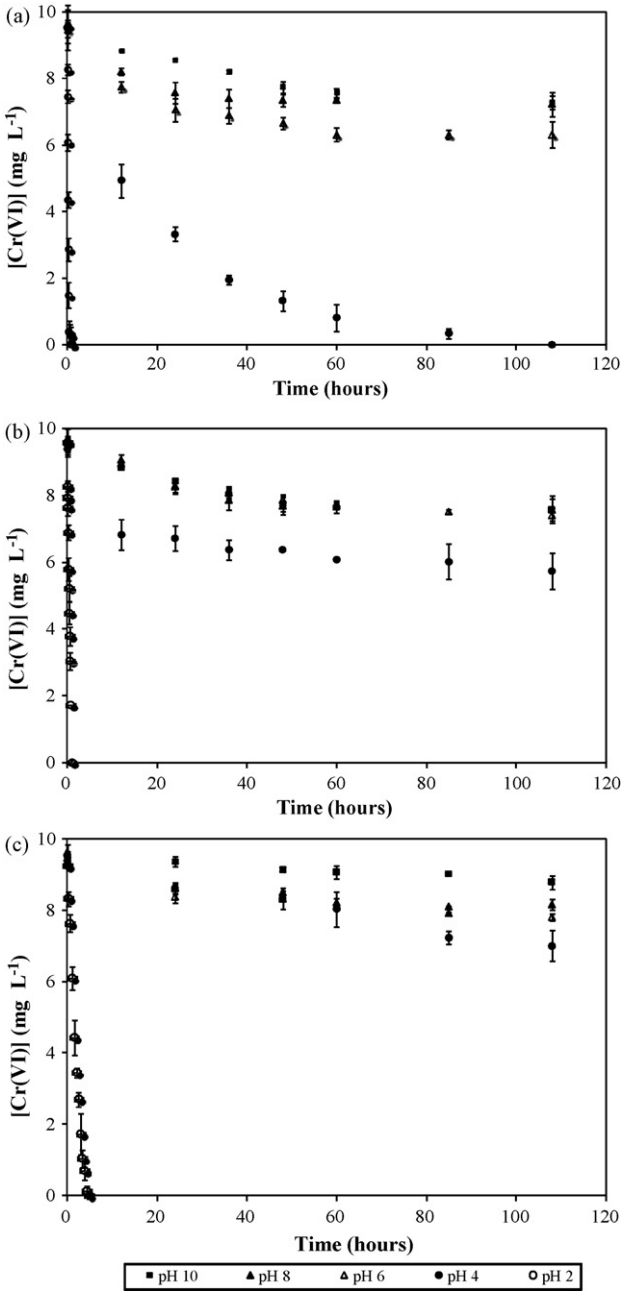

Fig. 3. Cr(VI) concentration at a given point in time, at different pH conditions. (a) Cr(VI) aqueous solution contact with Cu–Fe plates and (b) Cr(VI) aqueous solution contact with Fe plates. Initial Cr(VI) concentration of 10 mg L^{-1}.

rate. At pH 4, the iron and copper plates achieved respectively a 40% and 30% reduction after 100 h of contact time whereas the copper–iron bimetallic galvanic system achieved almost 100% in the same time. However, in all systems the amount of Cr(VI) reduced decreased at higher pH values. Similar results have been reported using electrochemical methods in which the reduction rates are fastest and most significant under acidic conditions, slower at neutral pH and slowest and least significant under alkaline conditions. At high pH, less than 15% of Cr(VI) is typically reduced [17].

As shown in Fig. 4, all systems completely reduce the hexavalent chromium in the solution at pH 2. However, the bimetallic galvanic system completes the reduction in the shortest time: 25 min for the copper–iron plates, 50 min for the iron plates and 290 min for copper plates.

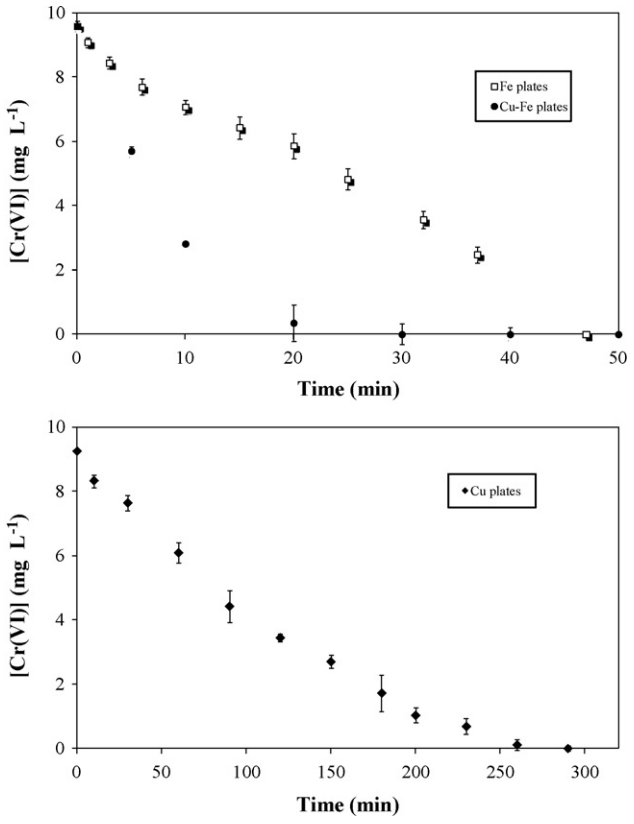

Fig. 4. Cr(VI) concentration at a given point in time at pH of 2. Initial Cr(VI) concentration of 10 mg L^{-1}.

The batch results were fitted to zeroth-, first- and second order kinetic models to calculate the kinetic constants and correlation coefficients by nonlinear regression with *Statistica 8.0*. At pH 2, the iron and the copper–iron bimetallic systems showed good correlation with the models with correlation coefficient values of 0.9900 for the iron system in zeroth order, 0.9935 for the copper–iron galvanic system in first order and 0.9899 for the copper system in first order. The iron and copper–iron systems under neutral and basic conditions exhibited low correlations coefficients of around 0.7. Under neutral and basic conditions the copper systems also show correlations of around 0.9.

Fig. 5 shows the decrease in Cr(VI) and the increase in Cr(III) and Cu ions using the copper–iron galvanic system. The changes in chromium and copper concentrations fit first order kinetics with good correlations: 0.9935 for Cr(VI), 0.9920 for Cr(III), and 0.9971 for Cu.

Both iron and the copper–iron galvanic systems produce iron ions, but at different rates. As shown in Fig. 6 with the kinetic modeling, the bimetallic system produces significantly more ions than the iron system. The correlation coefficients of the kinetic models are 0.9868 for the iron system in first order and 0.9953 in zeroth

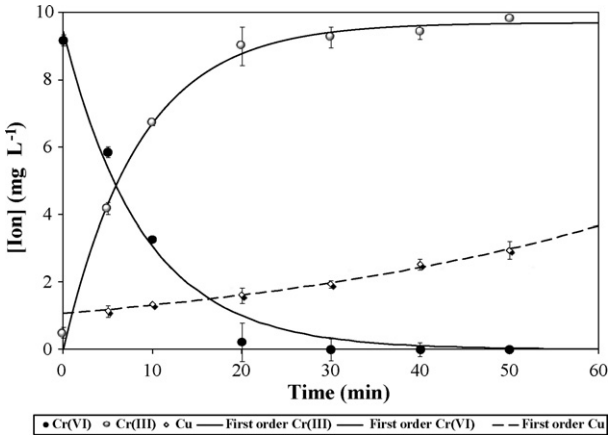

Fig. 5. Ion concentration of Cr(VI), Cr(III) and Cu at a given point in time, pH 2. Initial Cr(VI) concentration of 10 mg L^{-1}.

order for the copper–iron galvanic system. All kinetic values of the copper–iron system are listed in Table 1.

The mechanism of Cr(VI) reduction in the copper–iron galvanic system can be explained in terms of the optimized production of Fe^{2+} from the iron anode due to the potential difference that exists between the two metals immersed in a conductive solution. So, when the iron and copper plates are placed in contact this potential difference produces a flow of electrons between them enhancing the corrosion of the anode metal [18]. The reactions in the system are described below. Eq. (3) and (4) correspond to iron oxidation and hydrogen production at the anode and cathode. Eq. (5) is the global reaction that takes place in solution.

$$Fe^0 \rightarrow Fe^{2+} + 2e^- \quad (3)$$

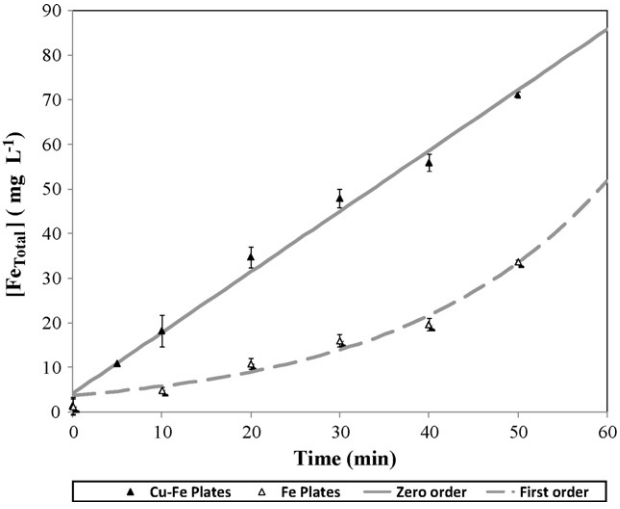

Fig. 6. Total Fe production in the Fe and galvanic Cu–Fe systems.

Table 1
Kinetic constants for the reduction of Cr(VI), zeroth-, first-, and second order models by bimetallic system.

	Zeroth order			First order		
pH 2 Cu–Fe	K_0 mg L^{-1} h^{-1}	C_e mg L^{-1}	r^2	K_1 h^{-1}	C_e mg L^{-1}	r^2
Cr(VI)				0.1122	9.4340	0.9935
Cr(III)				0.1176	9.7021	0.9920
Cu				−0.0206	1.0711	0.9971
Fe	−1.3602	4.2176	0.9953			

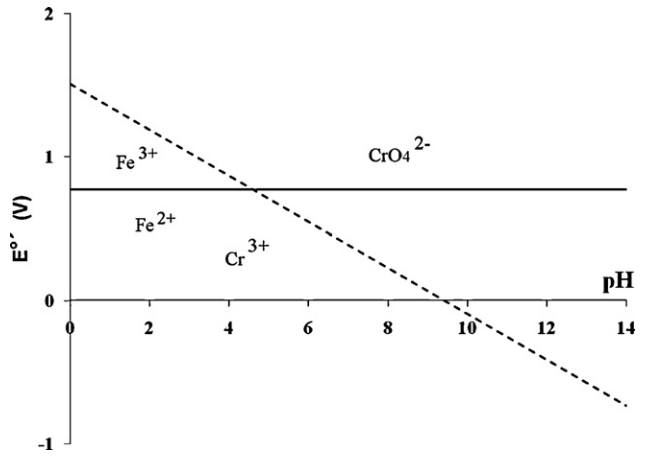

Fig. 7. Diagram of $E^{\circ\prime}$ as function of pH for (—) Fe(III)/Fe(II) and (- -) Cr(VI)/Cr(III) systems.

$$2H^+ + 2e^- \rightarrow H_2 \quad (4)$$

$$7H^+ + 3SO_4{}^{2-}HCrO_{4(aq)}{}^- + 3Fe_{(aq)}{}^{2+} \rightarrow Cr_{(aq)}{}^{3+} + 3Fe(SO)_{4(aq)}{}^+ + 4H_2O \quad (5)$$

Several studies have reported similar behavior in iron. Magnetite has been shown to reduce substantial amounts of Cr(VI) under acidic and neutral conditions, but less than 20% in basic solution [22]. Ferrite nanoparticles have also been used for Cr(VI) reduction with a sharp decrease in effectiveness as the pH increased from 2 to 9.3 [23]. Furthermore, the kinetics of Cr(VI) reduction by scrap iron indicated a very fast reduction in acidic conditions (pH 2), but much slower when the pH increased to 7, which was attributed to probable co-precipitation of mixed Fe(III)–Cr(III)hydroxides passivating the surface [24]. More recently, an investigation of the reduction of hexavalent chromium by waste slag generated from the iron industry found that the reduction rate of Cr(VI) was strongly pH-dependent from 2 to 6: the chromium was completely reduced in 20 min at pH 2, but only 17% at pH 4 in 300 min [25].

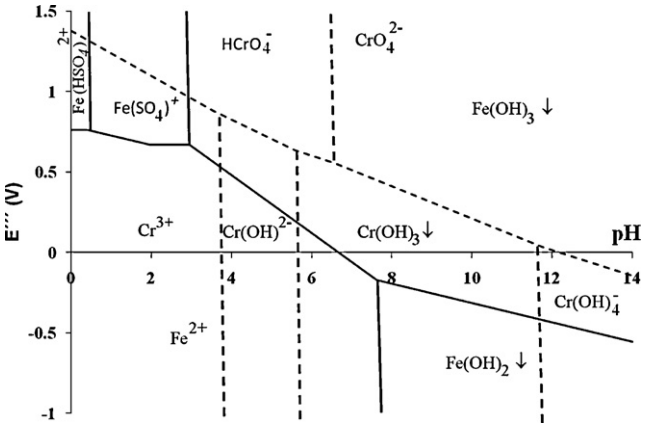

Fig. 8. Diagram of $E^{\circ\prime\prime}$ as function of pH for Fe(III)/Fe(II) (—) and Cr(VI)/Cr(III) (- -) at $pSO_4 = 2.3$, $p\text{Fe} = 2.27$ (300 ppm) and $p\text{Cr} = 2.71$ (100 mg L^{-1}).

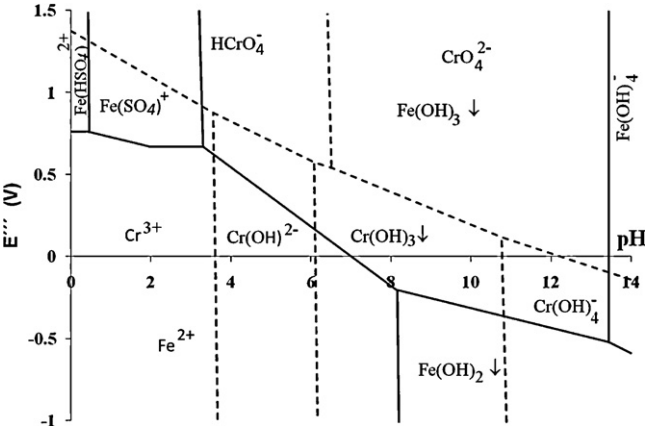

Fig. 9. Diagram of $E^{\circ\prime\prime}$ as function of pH for Fe(III)/Fe(II)) (—) and Cr(VI)/Cr(III) (- -) at $pSO_4 = 2.3$, $p\text{Fe} = 3.27$ (30 ppm) and $p\text{Cr} = 3.72$ (10 mg L^{-1}).

3.3. Thermodynamic explanation of Cr(VI) reduction under acidic conditions

The Cr(VI) reduction reaction depends on the pH. The chromium half reaction (6) indicates that protons are required for the reduction, but not for the iron (7) oxidation.

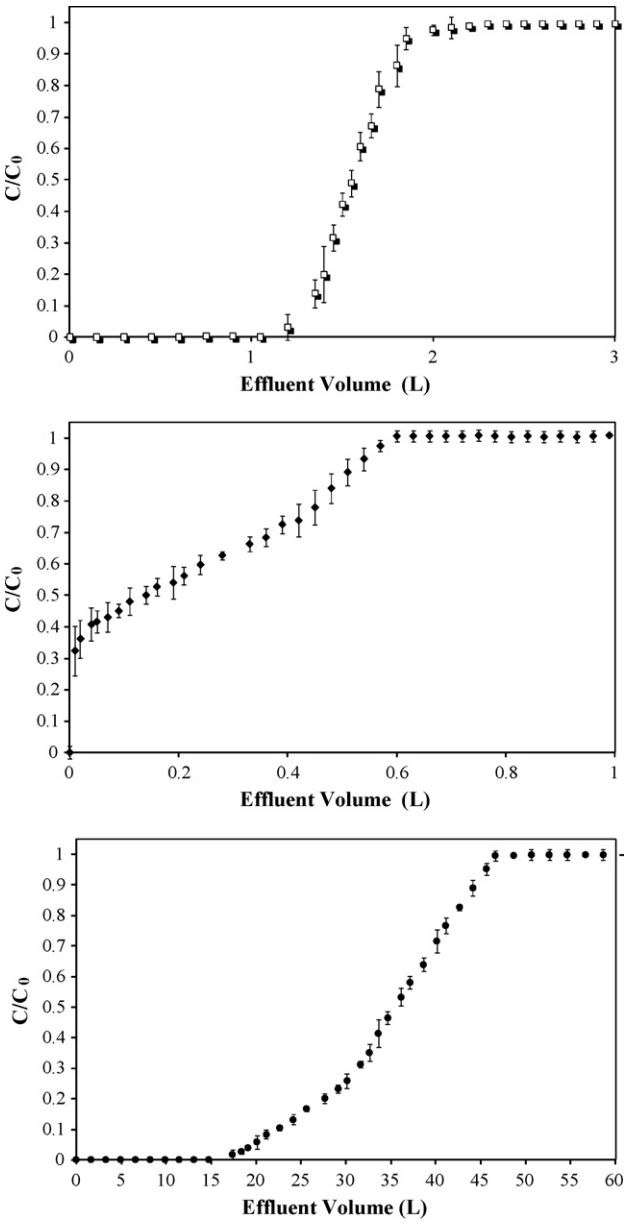

Fig. 10. Breakthrough curves of Cr(VI) reduction as a function of volume at pH 2. (□) Iron system, (♦) copper system and (●) copper–iron galvanic system.

$$3e^- + 7H^+ + HCrO_4^- \leftrightarrow Cr^{3+} + 4H_2O \quad (6)$$

$$SO_4^{2-} + Fe^{2+} \leftrightarrow Fe(SO_4)^+ + 1e^- \quad (7)$$

Fig. 7shows the Pourbaix diagram of the redox pairs Fe(III)/Fe(II) and Cr(VI)/Cr(III). The potential values of each of the species are presented at the different pH values and indicate if the reaction proceeds spontaneously. At pH values from 0 to 4.6 the oxidation potential of Cr(VI) is greater than the reduction potential of Fe(II). As shown in Eq. (8), the equilibrium constant depends on the potential difference value and indicates the spontaneity of the reaction ($K > 1$ indicates spontaneous reaction). For example, at pH 2 the value of the K is $10^{20.8}$, whereas at pH 10 it is $10^{-43.2}$.

$$K' = 10^{(n(E'_{ox} - E'_{red}))/0.06} \quad (8)$$

If we consider our experimental conditions of $pSO_4 = 2.3$, $pFe = 2.27$ and $pCr = 2.71$, the Pourbaix diagram changes since new chemical species are taken into account as well as the insoluble species. In Fig. 8, all of the chemical species are presented as a function of pH. It is significant that the reductant and oxidant lines do not cross; this implies that the potential of the oxidant is always greater than the reductant. Therefore, the Cr(VI) reduction reaction is thermodynamically possible at any pH value. However, at a pH value of 3.0 for iron and 5.5 for chromium insoluble species of both metals appear.

In Fig. 9, the same diagram is presented for a concentration of 10 ppm of chromium. The trends of Figs. 8 and 9 are quite similar except that at lower Chromium concentration, the solubility increases and $Fe(OH)_4^-$ appears.

3.4. Continuous flow systems

The Cr(VI) reduction by iron, copper and copper–iron packed columns are presented in the form of breakthrough curves in Fig. 10. The analysis of these packed columns was based on the development of effluent concentration-volume curves referred to as breakthrough curves. The curves are obtained by passing a solution with an initial concentration C_0 through the packed bed. As the flow continues the packed bed becomes saturated, at which

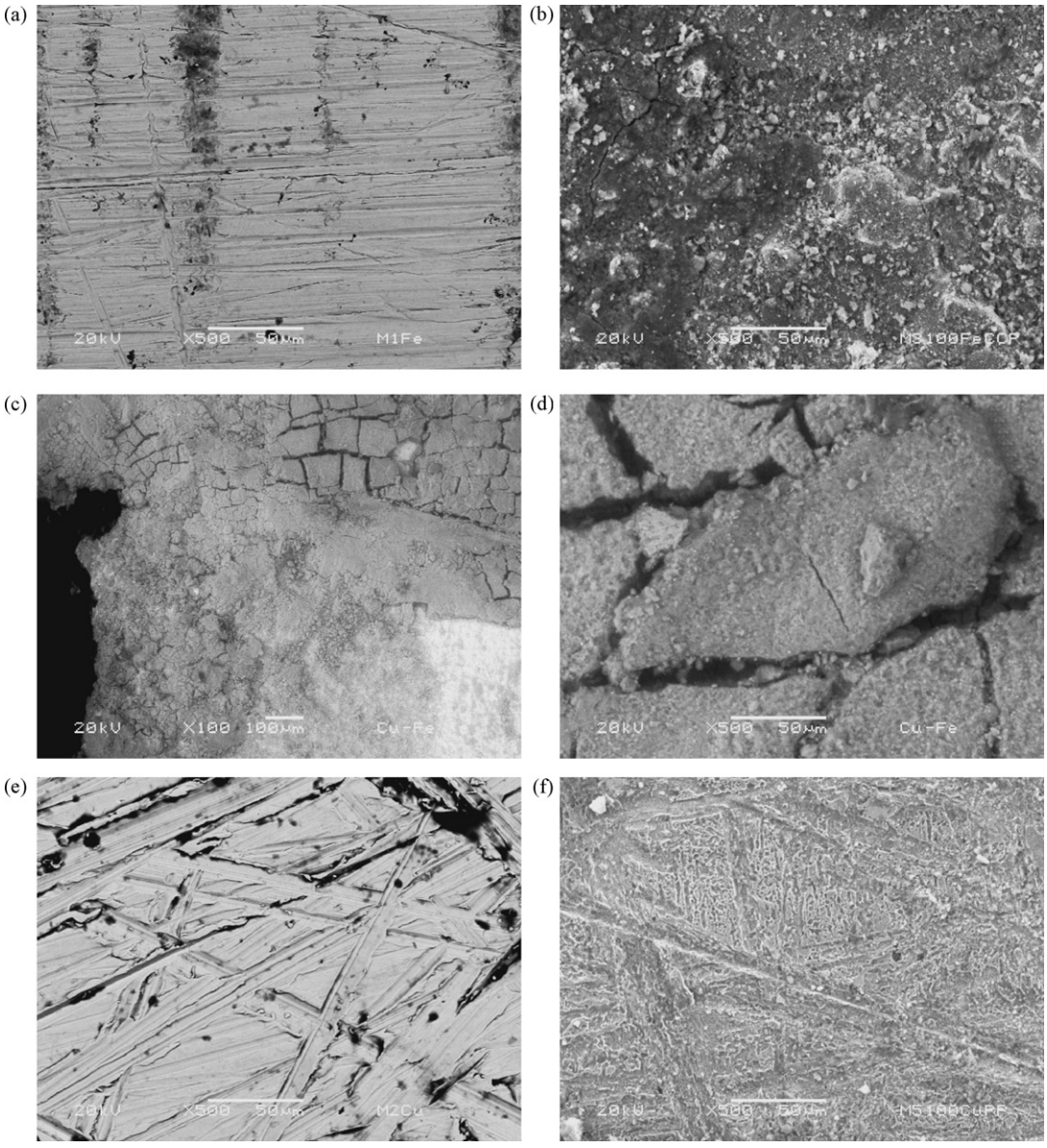

Fig. 11. SEM images of plate surfaces: Fe system plate before (a) and after (b) exposure and Cu–Fe system Fe plate after (c and d) and Cu plate before (e) and after (f) exposure.

Table 2
Service time of breakthrough curves of Cr(VI) reduction by iron, copper–iron and copper packed systems.

System	Q (mg cm^{-2})	Exhaustion time (min)	Service time (min)
Cu–Fe	9.5890	46,127	17,000
Fe	0.1269	2200	1000
Cu	0	600	0

point the solute first appears in the effluent stream. As the flow continues, the concentration in the effluent also increases. A breakpoint (maximum allowable) concentration is typically designated and the time to reach that level is called the service time. The packed bed becomes exhausted when the effluent concentration reaches a maximum value of C_0 and the time to reach this is designated the exhaustion time.

The results show that in the iron packed column, the Cr(VI) was completely reduced for the first 0.7 L of solution, with a service time of 1000 min, then lost effectiveness as more volume passed through the column, reaching exhaustion after a total of 2.2 L passed at 2200 min.

In the copper packed column, the Cr(VI) was never completely reduced. There was a high concentration in the first 0.01 L of effluent, so the service time is 0 min. The packed column completely lost effectiveness after a total of 0.6 L, reaching an exhaustion time of 600 min.

In the case of the galvanic copper–iron packed column, the Cr(VI) was completely reduced for the first 16 L followed by a slow, continuous increase in Cr(VI) concentration in the effluent. The service time for this system was found to be 17,000 min. Finally, the total volume required to reach the maximum capacity Q of the column was about 46 L with an exhaustion time of 46,127 min.

Table 2 lists the service and exhaustion times for each system. The capacity Q (mg cm^{-2}) at complete exhaustion was determined by the Metcalf–Eddy method [26]. This capacity represents the amount of Cr(VI) treated per unit weight/area of iron when the bed packed is at equilibrium with the initial concentration of Cr(VI). The breakthrough capacity was calculated as a function of the flow rate, influent and effluent concentrations, and breakthrough time.

The galvanic copper–iron system has a reduction capacity Q of 9.5890 mg Cr(VI) cm^{-2} iron, whereas iron alone only has a capacity of 0.1269 mg Cr(VI) cm^{-2} and copper has a capacity of zero.

3.5. Characterization of iron and copper–iron plates

3.5.1. SEM/EDS

After the Cr(VI) reduction process, the dried Fe and Cu plates were examined using SEM to establish a means of comparison regarding the effect of increasing iron corrosion rate of the copper–iron packed column, as shown in Fig. 11. The surface morphologies of the iron and copper plates before the Cr(VI) reduction (Fig. 11a and e) are continuous and homogeneous surfaces. However, an oxide layer forms on the surface of the iron system plates afterwards (Fig. 11b). This effect is also observed on the iron plates of the copper–iron packed column, but to a greater extent and more inconsistently (Fig. 11c) with some areas being very intense (Fig. 11d). The coating phenomenon is not observed on the copper plates due to the effective cathode protection by iron (Fig. 11f.).

After the SEM images were taken, the plates were also analyzed by EDS to determine the composition of the surface of the plates. The EDS spectra presented in Fig. 12(a) and (b) show the semi-quantitative elemental composition of the surface of the plates. As expected, the surface of the plate from the iron system is predominately iron and oxygen, with some precipitated chromium. The coating on the iron plate from the bimetallic system also has iron, oxygen, and chromium, but there is also a large amount of copper. This copper on the iron plate is likely due to the electrochemical reaction of the copper ions in solution with the iron surface, much the same as an iron nail placed in copper sulfate will acquire a metallic copper coating.

3.5.2. XRD

The XRD spectra (Fig. 13) of the powdered coatings from the iron plates from both systems show diffraction peaks indicative of iron oxides and hydroxides. The samples were identified as a mixture of iron oxides (magnetite and maghemite) and iron hydroxides (goethite and lepidocrocite). While the bimetallic iron plate did have metallic copper, there were no copper oxides or hydroxides.

In aqueous solution the iron plates interact with the OH^- naturally present in the water. Of course, the predominance of given compounds depends on the medium's pH. Consequently, the variety of Fe(II) or Fe(III) hydroxides formed depends on the pH. So, from SEM and XRD analyses of iron and iron bimetallic plates, there is no doubt that there was an effect on the surface due to the formation of insoluble species. The nature of these compounds, which coat the surface, leads to an increase electrical resistance of the electrochemical system because they are non-conducting compounds [27].

The passivation phenomenon has been observed for redox processes involving Fe(0) where it was coated with a thin oxide skin consisting mostly of magnetite. The redox process converted this to iron(III)–chromium(III) hydroxide, preventing electron transfer from deeper layers. At high Cr(VI) concentrations the passivation could be due to the precipitation of a sparingly soluble solid (such as a mixed Cr(III)–Fe(III) precipitate) or by a depletion of available Fe(II) within the structure [22].

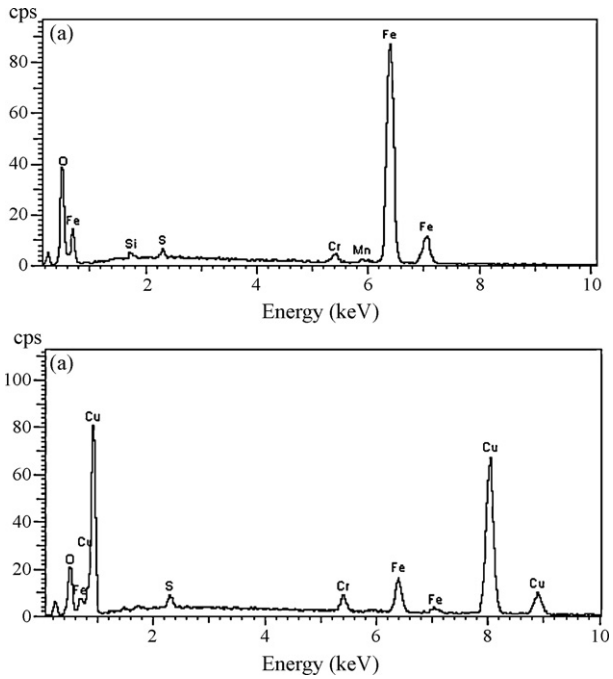

Fig. 12. EDS analyses of iron and copper–iron plates.

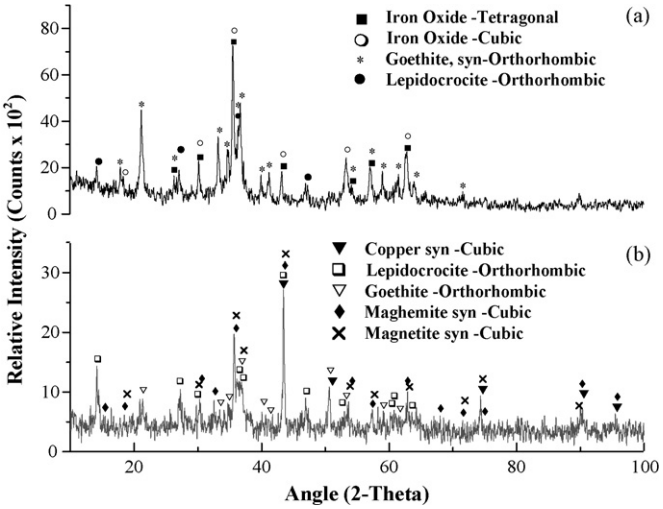

Fig. 13. XRD patterns of powder residues of (a) iron and (b) copper–iron plates.

4. Conclusions

A bimetallic galvanic system is capable of reducing Cr(VI) present in aqueous solution. The main advantages over traditional methods include no energy or chemical input into the system and lower sludge generation. The optimal conditions of pH 2 and a 3.5:1 ratio of copper to iron surface areas determined in batch studies allow 100% Cr(VI) reduction in about 25 min. Continuous column studies indicate that the galvanic copper–iron system has a reduction capacity of 9.5890 mg Cr(VI) cm^{-2} iron whereas iron alone only has a capacity of 0.1269 mg Cr(VI) cm^{-2}. Iron plates are used as the sacrificial electrodes in the system, whereas the copper can be reused. The exhausted plates were analyzed by SEM, EDS, and XRD to determine the mechanism and the surface effects, principally surface fouling due to iron oxides and hydroxides on the iron plates in both systems.

Acknowledgments

The authors wish to acknowledge the support given by the Centro de Investigación en Química Sustentable UAEM-UNAM (Project UAEM 2425/2007U) and by the Instituto Nacional de Investigaciones Nucleares (Project ININ-CB-703). Support from CONACYT and supporting research by SNI are greatly appreciated.

References

[1] M. Stoepler, Hazardous Metals in the Environment Techniques and Instruments in Analytical Chemistry, Elsevier, New York, 1992, p. 73.
[2] J. Gaulhofer, V. Bianchi, Chromium Metals and their Compounds in the Environment, VCH, Whenheimer, 1991, p. 30.
[3] R. Cespón-Romero, M. Yebra-Birrum, M. Bermejo-Barrera, Preconcentration and speciation of chromium by the determination of total chromium and chromium(III) in natural waters by flame atomic absorption spectrometry with a chelating ion-exchange flow injection system, Anal. Chim. Acta 37 (1996) 327.
[4] C. Barrera-Díaz, M. Palomar-Pardavé, M. Romero-Romo, S. Martínez, Chemical and electrochemical considerations on the removal process of hexavalent chromium from aqueous media, J. Appl. Electrochem. 33 (2003) 61–71.
[5] J. Nriagu, E. Nioeber, Chromium in the Natural and Human Environments, Wiley Series, New York, 1988, p. 82.
[6] D.L. Sedlak, P.G. Chan, Reduction of hexavalent chromium by ferrous iron, Geochim. Cosmochim. Acta 61 (1997) 2185–2192.
[7] A. Lu, S. Zhong, L. Chen, J. Shi, J. Tang, X. Lu, Removal of Cr(VI) and Cr(III) from aqueous solutions and industrial wastewaters by natural clino-pyrrhotite, Environ. Sci. Technol. 40 (2006) 3064–3069.
[8] R.R. Patterson, S. Fendorf, M.J. Fendorf, Reduction of hexavalent chromium by amorphous iron sulfide, Environ. Sci. Technol. 31 (1997) 2039.
[9] I.B. Singh, D.R. Singh, Influence of dissolved oxygen on aqueous solutions Cr(VI) removal by ferrous ion, Environ. Sci. Technol. 23 (2003) 1347.
[10] A.B. Riveiro, E.P. Mateus, L.M. Ottosen, G. Bech-Nielsen, Electrodialytic removal of Cu, Cr, and As from chromate copper arsenate treated timber waste, Environ. Sci. Technol. 34 (2000) 781.
[11] O.T. Can, M. Bayramoglu, M. Kobya, Decolorization of reactive dye solutions by electrocoagulation using aluminum electrodes, Ind. Eng. Chem. Res. 42 (2003) 3391.
[12] K. Rajeshwar, J.G. Ibanez, G.M. Swaine, Electrochemistry and environment, J. Appl. Electrochem. 24 (1994) 1077.
[13] L.J.J. Janssen, L. Koene, The role of electrochemistry and electrochemical technology in environmental protection, J. Chem. Eng. 85 (2002) 137.
[14] S.A. Martínez, M.G. Rodríguez, C. Barrera, A kinetic model that describes removal of chromium VI from rinsing waters of the metal finishing industry by electrochemical processes, Water Sci. Technol. 42 (2000) 55–61.
[15] D. Golub, Y. Oren, Removal of chromium from aqueous solutions by treatment with porous carbon electrodes: electrochemical principles, J. Appl. Electrochem. 19 (1989) 211.
[16] F.J. Rodríguez, S. Gutiérrez, J.G. Ibanez, J.L. Bravo, N. Batina, The efficiency of toxic chromate reduction by a conducting polymer (polypyrrole): influence of electropolymerization conditions, Environ. Sci. Technol. 34 (2000) 2018–2022.
[17] F. Rodríguez-Valadez, C. Ortiz-Éxiga, J.G. Ibanez, A. Alatorre-Ordaz, S. Gutiérrez-Granados, Electrorreduction of Cr(VI) to Cr(III) on reticulated vitreous carbon electrodes in a parallel-plate reactor with recirculation, Environ. Sci. Technol. 39 (2005) 1875–1879.
[18] M.G. Fontana, Corrosion Engineering, McGraw-Hill Series in Materials Science and Engineering, Ed. Board, New York, 1986, p. 294.
[19] APHA, AWWA, Standard Methods for the Examination of Water and Wastewater, 19th ed., American Public Health Association, Washington, DC, 1995.
[20] A. Rojas-Hernández, M.T. Ramírez, J.G. Ibáñez, I. González, Construction of multicomponent Pourbaix diagrams using generalized species, J. Electrochem. Soc. 138 (1991) 365.
[21] A. Rojas-Hernández, M.T. Ramírez, I. González, Predominance-zone diagrams in solution chemistry: dismutation processes in two-component systems (M–L), J. Chem. Ed. 72 (1995) 1099.
[22] Y. He-Thomas, J. Traina-Samuel, Cr(VI) reduction and immobilization by magnetite under alkaline pH conditions: the role of passivation, Environ. Sci. Technol. 39 (2005) 4499–4504.
[23] J. Hu, I.M.C. Lo, G. Chen, Comparative study of various magnetic nanoparticles for Cr(VI) removal, Sep. Purif. Technol. 56 (2007) 249–256.
[24] M. Gheju, A. Iovi, Kinetics of hexavalent chromium reduction by scrap iron, J. Hazard. Mater. B 135 (2006) 66–73.
[25] D. Park, S.-R. Lim, H.W. Lee, J.M. Park, Mechanism and kinetics of Cr(VI) reduction by waste slag generated from iron making industry, Hydrometallurgy 93 (2008) 72–75.
[26] Metcalf & Eddy, Wastewater Engineering Treatment and Reuse, 4th ed., McGraw Hill, 2003, pp. 1138–1162.
[27] J. Baptiste, M. Romero-Romo, P. Morales-Gil, M. Palomar-Pardavé, Potentiostatic formation of anodic films on an API-type low-alloy steel immersed in aqueous media with different pH, in: M. Palomar-Pardavé, M. Romero-Romo (Eds.), Electrochemistry and Materials Engineering, 1st ed., Research Signpost, 2007, pp. 224–226.